Photolysis of Caged Phosphatidic Acid Induces Flagellar Excision in *Chlamydomonas*†

Joachim Goedhart and Theodorus W. J. Gadella, Jr.*

Laboratory for Molecular Cytology, Swammerdam Institute for Life Sciences, University of Amsterdam, Kruislaan 316, 1098 SM Amsterdam, The Netherlands

Received July 2, 2003; Revised Manuscript Received December 18, 2003

ABSTRACT: Phosphatidic (PtdOH) acid formation is recognized as an important step in numerous signaling pathways in both plants and mammals. To study the role of this lipid in signaling pathways, it is of major interest to be able to increase the amount of this lipid directly. Therefore, "caged" PtdOH was synthesized, which releases the biologically active PtdOH upon exposure to UV. Analysis of the product revealed that two 2-nitrophenylethyl (NPE) caging groups were coupled to the phosphate headgroup of PtdOH. To measure the quantum efficiency of uncaging, a fluorimetric assay, based on the notion that the NPE cage is an efficient quencher of pyrene fluorescence, was developed. Consequently, after NPE-caged PtdOH and (*N*-pyrene)-PtdEtn had been mixed in DOPC vesicles, the extent of photolysis of caged PtdOH can be quantified by monitoring the increase in pyrene fluorescence. Using this assay, a quantum yield of 9.6% was determined for the uncaging reaction. The swimming green alga *Chlamydomonas moewusii* deflagellates upon addition of PtdOH. This response was used to study the release of PtdOH *in vivo*. Algae incubated with caged PtdOH only arrested swimming after exposure to UV, indicative of PtdOH release. This effect was not observed in the absence of the caged compound or when a control caged compound (caged acetic acid) was added. Fluorescein diacetate staining was used to show that the cells remained viable after UV exposure. The anticipated effect of PtdOH release is confirmed by phase contrast images of UV-exposed algae showing excision of flagella. Together, these results show that caged PtdOH can be used to efficiently increase PtdOH levels, demonstrating that it is a promising precursor for studying PtdOH-dependent signaling.

Phosphatidic acid (PtdOH)[1] formation is recognized as an important step in numerous signaling pathways in both plants (*1*) and mammals (*2*). Phosphatidic acid can be produced via two pathways, either by the action of phospholipase D (PLD) on structural lipids or by the phosphorylation of diacylglycerol (DAG), which itself is a second messenger produced by the phospholipase C pathway (*3*). Formation of PtdOH can be monitored by TLC of ^{32}P-labeled phospholipids, and this method can be used to distinguish between the two pathways (*1*). However, the requirement of PtdOH for a certain signaling cascade cannot be determined from such studies. Therefore, the involvement of PtdOH in signaling cascades is mainly proven by studies using inhibitors, protein overexpression, or knockout experiments. A less often used, but direct, method is to add PtdOH to cells (*4*−*6*). Although this method has been shown to work, the incorporation of the phospholipid will be inefficient because of the negatively charged headgroup. Furthermore, in mammalian systems, it has been shown that the vast majority of externally added PtdOH is converted to DAG by phosphatases (*7*). Also, at least in mammalian cells, PtdOH is a ligand for cell surface receptors (*8*).

To protect the phospholipid against degradation and to transfer it across the membrane, the negatively charged phosphate group can be masked by derivatization to a hydrophobic moiety, which has to be removed once the molecule has entered the cell. Such an approach has been described for PtdIns(3,4,5)P_3, which was derivatized with acetoxymethyl esters, which are cleaved intracellularly by phosphatases (*9*). Alternatively, photolabile protecting groups can be used. The protecting groups of the so-called "caged" molecule can be specifically removed by UV illumination (*10*), releasing the biologically active molecule. This approach was used to produce photolabile precursors of second messengers such as Ins(1,4,5)P_3 (*11*, *12*), Ca^{2+} (*13*), and cGMP/cAMP (*14*). The main advantages of this strategy are the high spatial and temporal levels with which the release can be controlled (*15*).

When the green alga *Chlamydomonas moewusii* is challenged with the G-protein activator mastoparan, PLC and PLD are activated (*16*), both contributing to an increase in the level of phosphatidic acid. The algae also respond morphologically to mastoparan by deflagellation. Interestingly, it has been shown that addition of phosphatidic to the cells is sufficient to induce deflagellation within 30 s (*4*).

† This work was supported by a grant (to J.G.) from the Netherlands Organization for Scientific Research-Council of Chemical Sciences (CW-NWO) and a "van der Leeuw" grant (to T.W.J.G.) from the Netherlands Organization for Scientific Research (NWO).

* To whom correspondence should be addressed. Telephone: +31 20 525 6259. Fax: +31 20 525 6271. E-mail: Gadella@science.uva.nl.

[1] Abbreviations: BODIPY 558/568-C_{12}, 4,4-difluoro-5-(2-thienyl)-4-bora-3a,4a-diaza-*s*-indacene-3-dodecanoic acid; DAG, diacylglycerol; DMNB-fluorescein, 4,5-dimethoxy-2-nitrobenzyl-caged fluorescein; FDA, fluorescein diacetate; NAP, nitrosoacetophenone; NPE, 1-(2-nitrophenyl)ethyl; PLD, phospholipase D; PtdOH, phosphatidic acid; PtdCho, phosphatidylcholine; Pyr-PtdEtn, pyrene phosphatidylethanolamine; TLC, thin-layer chromatography.

10.1021/bi0351460 CCC: $27.50
Published on Web 03/18/2004

Deflagellation can easily be observed as a loss of the ability to swim. Therefore, in this study, we used this response to investigate whether UV exposure of caged PtdOH can release PtdOH *in vivo*. Furthermore, control experiments are presented in which the effect of UV exposure and the possibly toxic released cage are evaluated. Together, the results show that the photolabile PtdOH precursor can release PtdOH *in vivo*, without affecting cell viability.

MATERIALS AND METHODS

Materials. FDA, 1-pyreneacetic acid succinimidyl ester, DMNB-fluorescein dextran (MW of 10000), and BODIPY 558/568-C_{12} were from Molecular Probes (Leiden, The Netherlands). Lyso-PtdCho, phosphatidic acid (from egg yolk lecithin), PLD from *Streptomyces chromofuscus*, activated $Mn(IV)O_2$, hydrazine hydrate, and 2-nitroacetophenone were from Sigma-Aldrich (Zwijndrecht, The Netherlands), and dipalmitoylphosphatidylethanolamine was from Avanti Polar Lipids (Alabaster, AL). $K_3Fe(C_2O_4)_3$ was prepared according to the method described in ref *17*. Briefly, 3 volumes of 1.5 M $K_2C_2O_4$ was mixed with 1 volume of 1 M $FeCl_3$. The mixture was stored in the refrigerator overnight, and the resulting crystals were recrystallized two times from water.

Biological Material. C. moewusii cells were cultured and prepared for experiments as described in ref *4*.

Synthesis of PtdCho with a BODIPY 558/568-C_{12} Acyl Chain. Acylation of 5 μmol of lyso-PtdCho was performed as reported previously (*18*) by reacting with the anhydride from 10 μmol of BODIPY 558/568-C_{12} prepared in dry $CHCl_3$ (*19*). Purification of the fluorescent PtdCho was carried out on CM-cellulose (*20*), from which the product eluted at 4% methanol as verified by TLC.

Synthesis of PtdOH from PtdCho by PLD. When PLD from cabbage was used, PtdCho was dissolved in 200 μL of ether which was added to 200 μL of 100 mM acetate buffer (pH 5.6) containing 100 mM $CaCl_2$ and 5 units of PLD. After incubation at 30 °C for 90 min, the ether was evaporated and the lipids were extracted with $CHCl_3$/MeOH. Alternatively, when PLD from *S. chromofuscus* was used, the PtdCho was suspended in 50 mM Tris (pH 8.0) and 10 mM $CaCl_2$ and incubated for 60 min at 37 °C in the absence of ether.

Synthesis of Pyr-PtdEtn. To synthesize PtdEtn with a pyrene linked to the free amino group (see Figure 3A), 0.5 mg of pyreneacetic acid succinimidyl ester, 1.5 μL of triethylamine, and 1.5 mg of PtdEtn were mixed in 500 μL of $CHCl_3$. The product had a typical pyrene absorbance (λ_{max} = 342 nm in EtOH) and emission spectrum (λ_{max} = 375 nm in EtOH). The solvents were evaporated, and the product was used without further purification.

Caged Compounds. The precursor 2-nitroacetophenone hydrazone was prepared as described previously (*21*, *22*). For a caging reaction, a 10-fold excess of 2-nitroacetophenone hydrazone was dissolved in chloroform, after which 8 molar equiv of MnO_2 was added. After being stirred vigorously for 5 min, the red solution was filtered through silanized glass wool. This solution was added to a chloroform solution of phosphatidic acid and incubated for at least 30 min. Subsequently, the solution was applied to a silica column from which the caged PtdOH was eluted with chloroform. Similarly, caged fatty acid was prepared. To prepare caged acetic acid (NPE-Ac), a 40-fold excess of glacial acetic acid was added to 1-(2-nitrophenyl)diazoethane which immediately turned yellow. Unreacted acetic acid was removed by extracting the chloroform solution with water.

Assessment of Uncaging. Phospholipid stocks were evaporated to give a total amount of 100 nmol [0.1 mol % Pyr-PtdEtn, x% caged phospholipid, and (99.9 − x)% DOPC]. To the lipid mixture was added 1 mL of PBS, and this mixture was sonicated for 1 min at an output of 40 W using a Branson (Danbury, CT) B-12 tip sonifier. The total volume was adjusted to 1.5 mL, and this was transferred to a cuvette. While being continuously stirred, the sample was illuminated with 365 nm (slit of 10 nm) light from a 75 W xenon arc lamp in a PTI (Lawrenceville, NJ) fluorimeter. At 10 min time intervals, the pyrene fluorescence (at 383 nm) was quantified by brief (3 s) excitation at 342 nm (slit of 10 nm).

By fitting the pyrene fluorescence increase according to eq 1 (see the Appendix), we determined the photorelease rate (k):

$$F'(t) = \frac{1}{1 + 2K_{Q_3}c_0 + c_0(K_{Q_2} - 2K_{Q_3})e^{-kt}} \qquad (1)$$

where $F'(t)$ is the fluorescence relative to unquenched pyrene, c_0 is the initial surface concentration of NPE_2-PtdOH, K_{Q_2} is the quenching constant of NPE_2-PtdOH, and K_{Q_3} is the quenching constant of nitrosoacetophenone (the product released after uncaging).

The quantum yield of uncaging (φ) is defined as the number of molecules photoreleased per second (n) divided by the number of photons absorbed per second (f). The number of photoreleased molecules generated per second (n) is determined by the rate of uncaging (k), the concentration (c), and volume (V) of the uncaging reaction medium according to

$$n = kcVN_A \qquad (2)$$

in which N_A is Avogadro's number.

The number of photons absorbed per second (f) is the product of the number of administered photons to induce uncaging per second (or flux) (ϕ) and the fraction of these photons that are absorbed. The fraction of absorbed photons follows from Lambert−Beer's law and relates to the molar extinction coefficient (ϵ), the length (l) of the reaction vial (parallel to the light), and the concentration of the caged molecule (c).

$$f = \phi(1 - 10^{-\epsilon cl}) \qquad (3)$$

The quantum yield is the quotient of eqs 2 and 3:

$$\varphi = \frac{kcVN_A}{\phi(1 - 10^{-\epsilon cl})} \approx \frac{kVN_A}{\phi \ln 10\, \epsilon l} \quad (\text{if } \epsilon cl < 0.01) \qquad (4)$$

It is noteworthy that at a low concentration c, where the absorbance A (=ϵcl) becomes <0.01, the calculation of the quantum yield φ is independent of the concentration of caged molecules.

For uncaging of DMNB-fluorescein dextran, a final concentration of 30 nM in 1.5 mL of PBS was used, and uncaging was monitored by measuring the fluorescence emission at 520 nm upon excitation at 480 nm.

Determination of the Photon Flux. The photon flux in the PTI fluorimeter at 365 nm (slit of 10 nm) was determined by ferrioxalate actinometry. A fresh solution of 0.006 M $K_3Fe(C_2O_4)_3$ in 0.5 M H_2SO_4 was exposed for 60 s while being continuously stirred. The UV-induced formation of Fe^{2+} was assayed by 1,10-phenanthroline as described previously (*17*). Briefly, 100 μL of the ferrioxalate solution was mixed with 400 μL of 0.1% (w/v) 1,10-phenanthroline, 50 μL of acetate buffer (0.82 g of NaAc and 100 μL of concentrated H_2SO_4 in a final volume of 10 mL), and 450 μL of H_2O. After incubation for 1 h, Fe^{2+} was assessed at 510 nm with nonexposed ferrioxalate as a control (ϵ = 11 100 M^{-1} cm^{-1}) and converted to the number of photons per second using a quantum yield of 1.21 (*17*).

Photorelease with a Microscope. The microscope setup has been described previously (*23*). Light from a 100 W mercury lamp was passed through an excitation band-pass 365HT25 filter (Omega, Brattleboro, VT) and reflected onto the sample using a 430DCLP dichroic mirror. Exposure was at a magnification of 20×, after which an image was acquired at a magnification of 10× with a Quantix CCD camera (Photometrics, Tucson, AZ) controlled by IPLab spectrum software (Signal Analytics, Vienna, VA). To achieve good statistics, the samples were illuminated for 5 min unless stated otherwise, inducing accumulation of a substantial amount of deflagellated algae in the exposed spot. To calibrate the position of UV exposure within the microscope field, 50 μg/mL DMNB-fluorescein dextran in 80% glycerol in a microcuvette with an internal diameter of 0.1 mm (VitroCom, Mountain Lakes, NJ) was exposed for 1 s, after which an image with fluorescein filter settings was taken immediately. The chlorophyll fluorescence of *C. moewusii* was acquired with 10-fold reduced excitation power and an LP610 emission filter. An integration time of 10 s for image acquisition was used to selectively image nonswimming cells, since the signal of swimming cells is blurred by their motion.

Image Processing. Image processing was done with NIH image version 1.62. Digital images were imported using the IPLab import macro. A threshold was applied to separate cells from the background, and the image was converted to a binary image in which cells were given a value of 1 and background a value of 0. This image was multiplied by the UV intensity distribution image (Figure 4A). The histogram of the multiplied image was divided by the histogram of the UV intensity image, yielding a histogram that correlates the probability of finding a cell with the intensity of UV light. Further details are discussed in the Results and Discussion.

RESULTS AND DISCUSSION

Caging of Phosphatidic Acid. Fluorescent PtdOH can be synthesized from fluorescent acyl chain-labeled phosphatidylcholine after PLD treatment (*24*). Therefore, we started with preparing fluorescent PtdCho by reacting lyso-PtdCho with the anhydride of BODIPY 558/568-C_{12}, which is purified on CM-cellulose and then treated with PLD to prepare fluorescent PtdOH. The preparation of BODIPY 558/568-C_{12}-labeled PtdOH by the action of PLD on fluorescent PtdCho typically yields >90% PtdOH (see lane A of Figure 2). This is used without further purification.

We have caged PtdOH by the addition of 1-(2-nitrophenyl)ethyl (NPE) moieties onto the free phosphate as reported by Williger et al. (*25*) by reacting PtdOH with 1-(2-nitrophenyl)diazoethane. The subsequent application of the caged compound to a silica gel column serves two purposes. First, the remaining 1-(2-nitrophenyl)diazoethane is inactivated by a reaction with the silica gel. Second, both the contaminants PtdCho and unreacted PtdOH bind to the column, whereas the caged PtdOH is eluted with chloroform. The purity of caged PtdOH is excellent as can be inferred from TLC (lane B of Figure 2). Similarly, natural PtdOH was caged and purified.

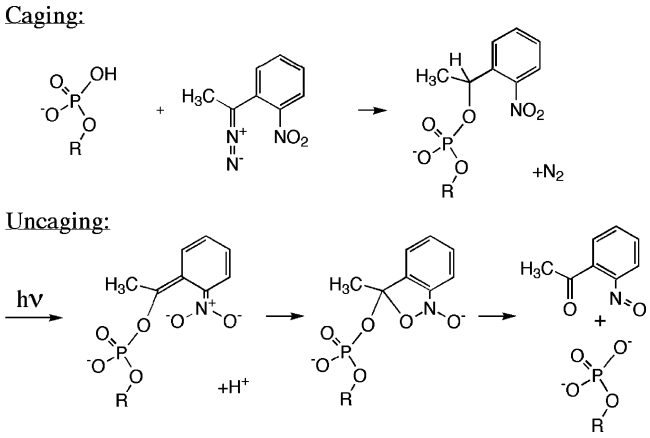

FIGURE 1: During caging, the phosphate group is derivatized by a reaction with 1-(2-nitrophenyl)diazoethane in $CHCl_3$ which yields the photosensitive NPE moiety. During uncaging, upon exposure to UV light (365 nm), an aci-nitro intermediate is formed, after which intramolecular transfer of the oxygen from the nitro group takes place which yields the original compound and the byproduct 2-nitrosoacetophenone. R is diacylglycerol for PtdOH.

Photolysis of Caged Phosphatidic Acid. Using fluorescent caged PtdOH, the photorelease of PtdOH *in vitro* can be easily evaluated by TLC analysis. When a sample of caged PtdOH is exposed to UV and subsequently run on a TLC plate, it is directly apparent that PtdOH is released from the caged compound (lane C of Figure 2). Another UV-induced compound is also present on the TLC plate after irradiation (close to the NPE-PtdOH spot, lane C), which was not present after prolonged exposure of caged PtdOH to UV, yielding only PtdOH (data not shown). If the UV irradiation was interrupted, the intermediate turned out to be stable for at least 1 day. This is remarkable since no stable intermediates are known for the photorelease of the NPE group (*21*). As the intermediate was observed for both BODIPY-labeled and natural PtdOH (data not shown), the intermediate is not related to the fluorescent label. Interestingly, in contrast to the intermediate, the product of the caging reaction (caged PtdOH) could not be detected by molybdate spray, which is used to detect phosphomono- and -diesters (not shown). These observations point out that we synthesized a phosphatidic acid bearing two cages (being a phosphotriester). This compound will be termed NPE_2-PtdOH, and its structure is shown in Figure 3A. Hence, the intermediate is the singly caged compound (NPE-PtdOH), as depicted in Figure 1. A kinetic analysis of the formation of the intermediate was performed by continuously exciting a sample of NPE-PtdOH in ethanol with 365 nm light in a fluorimeter. A sample was taken at the indicated time points and analyzed on TLC (see Figure 2). Clearly, the first (F1−F6) appearance of the intermediate can be observed, and later (F7) its subsequent disappearance and conversion into PtdOH.

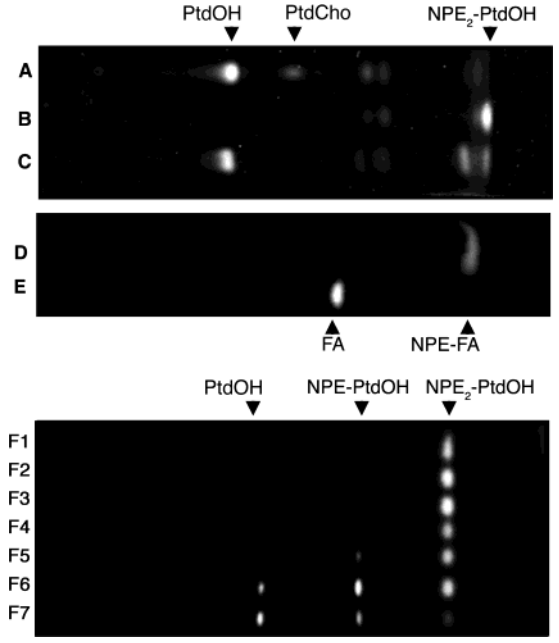

FIGURE 2: TLC analysis of the synthesis and photolysis of fluorescent caged PtdOH and fatty acid. (A) Fluorescent PtdOH produced by the action of PLD on BODIPY 558/568-C_{12}-labeled PtdCho. (B) Fluorescent caged PtdOH obtained after reaction of PtdOH with 1-(2-nitrophenyl)diazoethane and subsequent purification. (C) Release of PtdOH from caged PtdOH in an H_2O/EtOH mixture (1:1, v/v) after illumination with UV light (365 nm) for 1 min. (D) Fluorescent caged BODIPY 558/568-C_{12} obtained after reaction of the labeled fatty acid with 1-(2-nitrophenyl)diazoethane and subsequent purification. (E) Release of the BODIPY-C_{12} fatty acid from NPE-BODIPY 558/568-C_{12} in an H_2O/EtOH mixture (1:1, v/v) after illumination with UV light for 5 min. In lanes F1−F7, kinetic analysis of the uncaging reaction in EtOH was carried out; 20 μM purified fluorescent NPE_2-PtdOH was illuminated at 365 nm (slit of 10 nm) in a fluorimeter under continuous stirring, and aliquots were taken at 0, 1, 2, 5, 10, 30, and 60 min , respectively. Samples A−C were run in a $CHCl_3$/MeOH/25% NH_3/H_2O mixture (50:30:3:3, v/v/v/v) and samples D−F in a $CHCl_3$/MeOH/25% NH_3/H_2O mixture (45:35:8:2, v/v/v/v).

Novel Assay for the Quantification of the Uncaging Rate and Quantum Yield. Determination of the uncaging quantum yield usually involves laborious quantitative off-line HPLC analysis, in which the amount of caged precursor and caged product are quantified as a function of time (*22*), usually demanding a relatively large amount of the caged probe. We developed a new spectroscopic approach for measuring the extent of uncaging in real time which also allowed us to determine uncaging rates in model membranes. The approach is based on the notion that nitrophenyl derivatives are effective quenchers of pyrene fluorescence (*26*). Hence, by mixing NPE-caged lipids, and a trace of pyrene-labeled lipid in model membranes, we can directly monitor the extent of uncaging by measuring the concomitant increase in pyrene fluorescence (see Figure 3A). We found that headgroup-labeled PtdEtn was efficiently quenched by NPE_2-PtdOH. Pyrenylacyl-labeled lipids were less efficiently quenched (data not shown). To determine optimal conditions for the uncaging assay, various amounts of (nonfluorescent) NPE_2-PtdOH were incorporated in DOPC vesicles containing 0.1% Pyr-PtdEtn. At 365 nm (used for uncaging), pyrene is hardly excited, avoiding enhanced photolysis due to the transfer of energy from pyrene to the NPE cage.

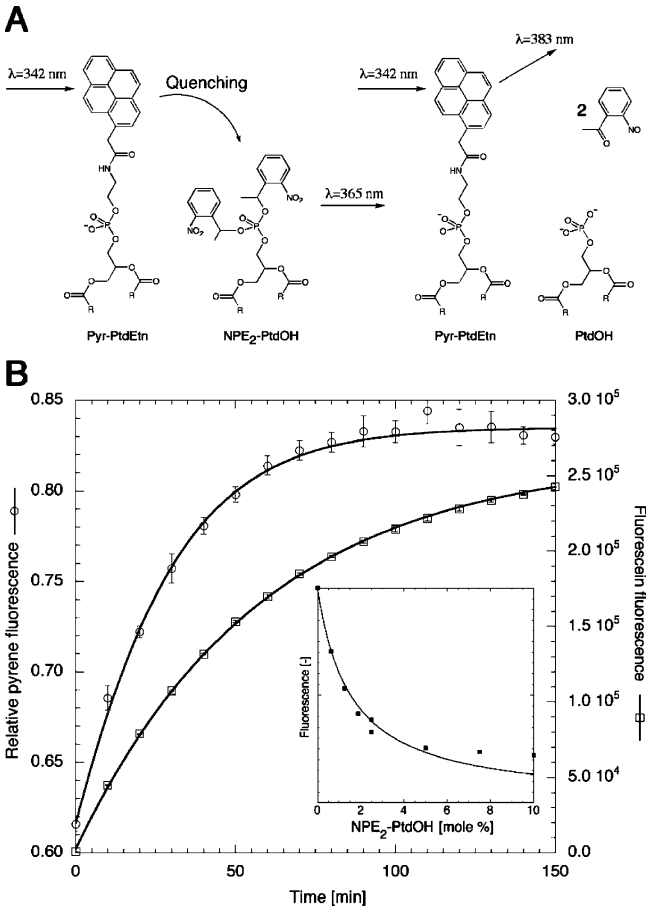

FIGURE 3: Assay for the real-time fluorimetric assessment of the uncaging of NPE_2-PtdOH. (A) A schematic presentation of the principle of the assay. Initially, Pyr-PtdEtn is quenched by the caged compound, and both are present in a small unilamellar vesicle. Upon photolysis at 365 nm, the cage is removed, and Pyr-PtdEtn is no longer quenched and will emit blue fluorescence. (B) Fluorescence increase of pyrene-PtdEtn and DMNB-fluorescein due to photolysis of NPE_2-PtdOH and DMNB-fluorescein, respectively. The samples were continuously exposed to 365 nm light in a fluorimeter, and at 10 min intervals, the fluorescence of pyrene (○) or fluorescein (□) was monitored. The observed fluorescence increase was fitted (—) as described in the text. The inset shows pyrene fluorescence as a function of the amount of quencher (NPE_2-PtdOH). The data were fit according to the formula for Stern−Volmer quenching (equation V from the Appendix). The fit for the NPE uncaging had a correlation coefficient of 0.9986, and we determined the following: $K_{Q_3} = 0.049$, $K_{Q_2} = 0.52$, and $k = 0.042$ min^{-1}. The other curve (for fluorescein) was fitted using a simple single exponential [$F/F_{max} = 1 - \exp(-kt)$], yielding a correlation coefficient of 0.9999 and a k value of 0.017 min^{-1}.

The inset of Figure 3B shows the fluorescence of Pyr-PtdEtn at various concentrations of NPE_2-PtdOH. Clearly, the pyrene fluorescence is increasingly quenched when the amount of caged PtdOH is increased. At surface concentrations of up to 5 mol % NPE_2-PtdOH, the quenching could be described by simple Stern−Volmer quenching (see eq V of the Appendix). A quench constant K_Q of 0.64 (mol %)$^{-1}$ was determined. For the determination of the rate of uncaging, 1 mol % NPE_2-PtdOH in the vesicles was used. When vesicles with both Pyr-PtdEtn and NPE_2-PtdOH were continuously excited at 365 nm, a clear increase in pyrene fluorescence was observed, which gradually leveled off, as shown in Figure 3B. It is of note that the time course of the uncaging reaction measured in this assay is similar to the

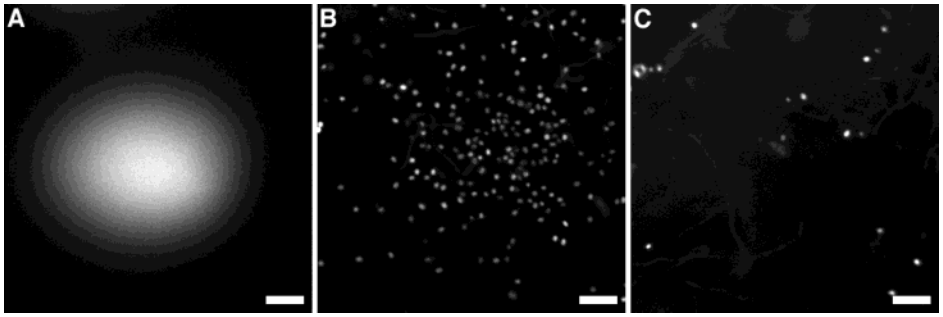

FIGURE 4: *In vivo* uncaging by spatially restricted UV exposure and subsequent fluorescence imaging. (A) UV-induced extent of uncaging image as estimated by the fluorescence that is induced due to uncaging of caged fluorescein-dextran in glycerol. (B) Immobilized *C. moewusii* loaded with 0.7 μM NPE_2-caged BODIPY 558/568-C_{12} PtdOH after uncaging for 5 min with UV. Accumulated cells were visualized by monitoring their chlorophyll autofluorescence. A 10 s integration time was used, resulting in selective imaging of nonswimming cells, since swimming cells are blurred because of their mobility. (C) Control uncaging after incubation with 25 μM NPE-Ac. All other conditions were identical to those described for panel B. Bars are 50 μm long.

time course observed for full uncaging of the fluorescently caged PtdOH as analyzed by TLC (Figure 2).

The curves were fitted to eq 1 (also see the Appendix), from which the rate of uncaging could be determined. As can be inferred from Figure 3B, the fit accurately describes the data ($R = 0.999$). Moreover, the value of K_Q for this fit was 0.52 (mol %)$^{-1}$, which is close to the value independently obtained from the quenching curve. From the fit, the rate of uncaging (k) was determined to be 7.0×10^{-4} s^{-1}/cage. Using an extinction coefficient (ϵ) of 500 M^{-1} cm^{-1} (*10*) and a photon flux of 5.7×10^{15} s^{-1} (determined by ferrioxalate actinometry), this yields an uncaging quantum efficiency of 9.6% according to eq 4. For comparison, the rate of uncaging of DMNB-fluorescein dextran was determined as well. This caged molecule is nonfluorescent. Upon photolysis, fluorescein is liberated, which can be simply quantified by measuring its fluorescence. In Figure 3B, the increase in fluorescein fluorescence is shown. A monoexponential fit of the data yields an uncaging rate of 2.85×10^{-4} s^{-1}, using an absorbance coefficient of 5000 M^{-1} cm^{-1} the uncaging quantum yield is 0.4%. The efficiency of uncaging is determined by the product of the quantum yield and the molar extinction coefficient. At 365 nm, these efficiencies are 48 and 20 M^{-1} cm^{-1} for caged PtdOH and caged fluorescein, respectively. The rather similar uncaging efficiencies allow the use of caged fluorescein to estimate the degree of uncaging of PtdOH in a microscope.

In Vivo Assay for the Photorelease of PtdOH. PtdOH is implicated as a second messenger in several plant responses (*4*). A relative well-characterized signaling process takes place when the green alga *C. moewusii* is exposed to mastoparan. The G-protein agonist elevates the level of PtdOH, thereby inducing the excision of its flagella. It has been shown that addition of PtdOH vesicles is sufficient to induce excision of the flagella (*4*). This response can be easily observed since after deflagellation the cells are unable to swim. Hence, by monitoring the mobility of the alga in the absence and presence of UV light and caged PtdOH, we have a convenient assay for studying the photorelease of PtdOH *in vivo*.

The extent of uncaging of the employed UV light in the sample was calibrated by illuminating a solution of caged (nonfluorescent) fluorescein, and subsequently taking an image of the uncaged and fluorescent fluorescein (Figure 4A). Typically, a 50% (of total) increase in fluorescence was observed after exposure to 365 nm light for 1 s. As the uncaging efficiencies of NPE_2-PtdOH and DMNB-fluorescein are within 1 order of magnitude at 365 nm (see above), we expect that under these illumination conditions the 50% increase of NPE_2-PtdOH is also uncaged. It is of note that the intensity of the UV light in the microscope at the specimen is several orders of magnitude higher than the UV intensity that is used in the fluorimeter assay. Consequently, the uncaging rates are proportionally higher in the microscope. Since the intrinsic photolysis rate (after absorption of the UV photon) of NPE cages on phosphate moieties ranges between 20 and 1000 s^{-1}, subsecond time resolution can be achieved with these caged molecules (*10*).

Next, swimming *C. moewusii* cells were observed under a microscope. Continuous illumination of the spots shown in Figure 4A with UV light did not impair the motility of untreated cells that crossed these spots. When the same experiment was carried out after application of 0.7 μM caged PtdOH to the *C. moewusii* cells, swimming was arrested specifically at the illuminated spots, indicating that both caged PtdOH and UV light were required and sufficient to stop the cells (Figure 4B). The photolysis of caged PtdOH yields a side product which is 2-nitrosoacetophenone. To investigate whether this compound might be harmful for the cells, a control experiment was performed in which either caged fatty acid or caged acetic acid (NPE-Ac) was used. As shown in Figure 4C, even when a 35-fold excess of NPE-Ac was used, no change in the swimming speed of the cells was observed upon illumination with UV, indicating that the side product is not responsible for the arrest of the motility. Similar results were obtained for the caged fatty acid (data not shown).

To determine the approximate exposure of the cells to the caged compound, we measured the swimming velocity, which is on average 75 μm/s [standard deviation of 8 μm/s ($n = 13$)]. As the spot diameter of the UV excitation is approximately 200 μm, on average cells will be exposed for 3 s, which is sufficient for the deflagellation response. Still, it could be observed that some cells could swim across the excitation spot, indicating that there is a time lag of a few seconds between uncaging and deflagellation. An explanation of the time lag would be that the doubly caged PtdOH needs two uncaging events before it becomes active. As 50% of the (also doubly caged) fluorescein is released within 1 s in the microscope, we assume that a substantial portion of

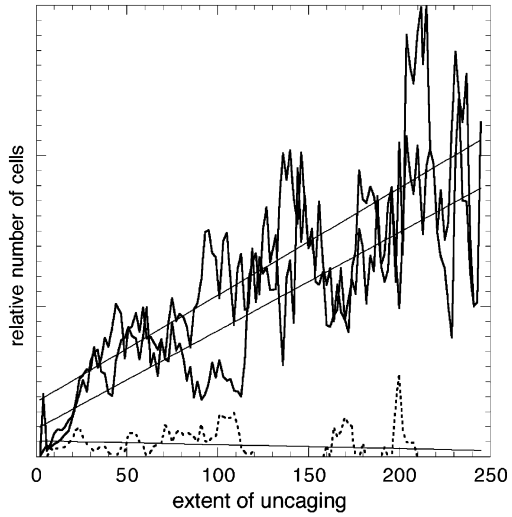

FIGURE 5: Histograms showing the probability of finding immobile cells as a function of the extent of uncaging. The straight line represents a linear least-squares fit through the data points. In the case of caged BODIPY 558/568-C_{12} PtdOH-loaded cells (straight lines), there is a positive correlation with the extent of uncaging, whereas no correlation (dashed line) is observed when cells are incubated with NPE-Ac.

NPE_2-PtdOH is converted into PtdOH within 1 s. Although we do not exclude a less than quantitative conversion in the 3 s exposure time, we think that it is more likely that this time lag reflects intermediate signal transduction between PtdOH generation and the final response.

The image shown in Figure 4B shows that the spot at which cells that are unable to swim accumulate correlates with the area with the highest extent of uncaging as shown in Figure 4A. To quantitatively relate deflagellation with the extent of uncaging, we applied an image correlation method. First, the images of cells (Figure 4B,C) are thresholded and converted to binary images, in which pixels corresponding to (nonmotile) cells are given the value of 1 and background pixels a value of 0. The binary image is multiplied with the extent of uncaging image. This yields an image in which the background has a value of 0 and cells have a pixel value corresponding to the extent of uncaging. A histogram of the intensities in this image represents the probability of finding a nonswimming cell as a function of the local extent of uncaging. This histogram, however, must be divided by the probability of finding a certain extent of uncaging, i.e., the histogram of the extent of uncaging distribution in Figure 4A. The normalized histogram shows the probability of finding a cell at a certain extent of uncaging. In the case of a random distribution of cells, there should be no correlation of the location of the cells with respect to the extent of uncaging. However, in the case of accumulation of cells in the UV-exposed areas, a positive correlation between the extent of uncaging and the number of cells is expected. The data of two experiments with caged PtdOH present and one control experiment are analyzed using this procedure. The results are shown in Figure 5. Clearly, a positive correlation between the extent of uncaging and the number of accumulated cells is seen for cells incubated with caged PtdOH, whereas no such trend is seen in cells incubated with NPE-Ac. Hence, the analysis routine is capable of extracting the PtdOH specific response and allows a quantitative comparison with control situations.

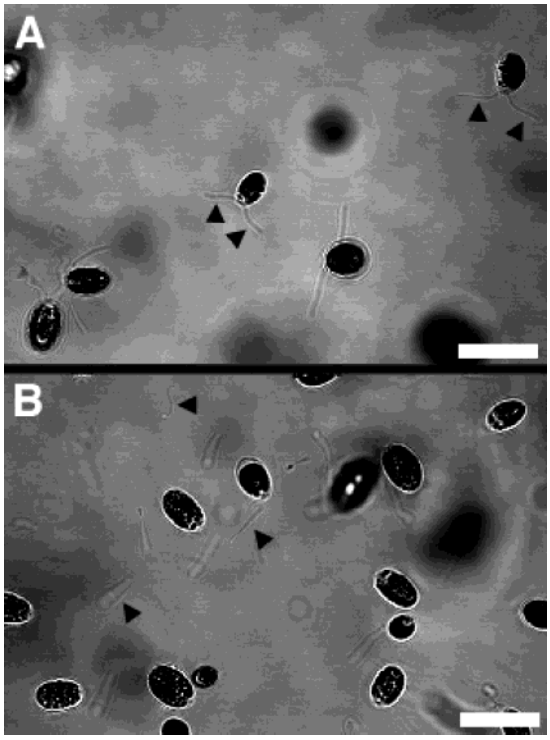

FIGURE 6: Release of PtdOH induces flagellar excision. In panel A is shown the phase contrast image of algae incubated with caged BODIPY 558/568-C_{12} PtdOH but not exposed to UV light. Few cells are immobilized, and clearly, these cells still carry both flagella as indicated with arrowheads. The phase contrast image of an exposed region (panel B) shows more cells that are nonmotile and that do not have their flagella. Even some excised flagella (arrowheads) can be distinguished in this image. Bars are 20 μm long.

The curve in Figure 5 suggests a linear relationship between the extent of uncaging and the deflagellation response. However, we do not want to draw any further conclusions from this seemingly linear behavior, given (i) the high signal-to-noise ratio in the curves (caused by the brief lag time between passage through the UV spot and deflagellation) and (ii) the fact that no actual UV light distribution was measured in the sample (this is very complicated since one needs to dissect the spatial light distribution from the spatial light detection efficiency through the microscope).

To estimate the sensitivity of the algae to the caged compound, a dilution series was made to determine the minimal amount of NPE_2-PtdOH necessary to observe the accumulation. The caged PtdOH was still active at concentrations down to 0.4 μM, whereas noncaged dioctanoyl-PtdOH required a concentration of 100 μM to induce deflagellation.

PtdOH Release Induces Flagellar Excision. The previous experiments have shown that UV exposure can release PtdOH *in vivo*, and that the algae arrest swimming due to PtdOH release. We anticipated that PtdOH release causes motility arrest due to flagellar excision. To check whether deflagellation is indeed occurring, higher-magnification phase contrast images were acquired for cells treated with caged PtdOH. Cells in nonexposed regions are compared to those in exposed regions. In Figure 6A, a phase contrast image of nonswimming cells in a nonexposed region is shown. These cells clearly carry both flagella, suggesting that the caged

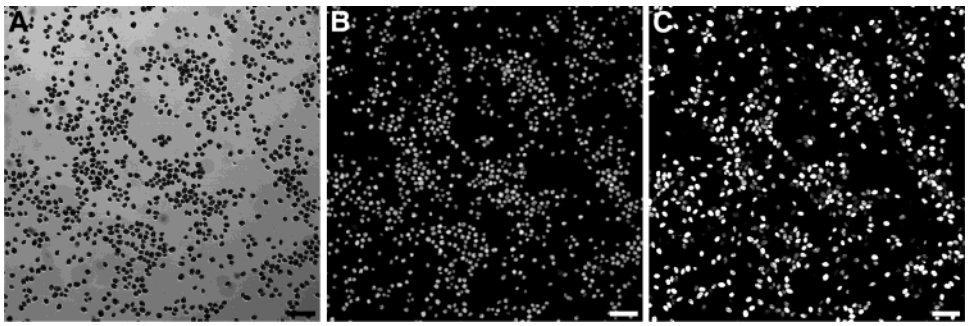

FIGURE 7: Viability of algae after UV exposure. After being incubated with caged BODIPY 558/568-C_{12} PtdOH and exposed to UV light for 5 min, the cells were tested for viability by measuring their ability to hydrolyze FDA (final concentration of 10 μM) into fluorescein. In panel A is shown the phase contrast image of immobilized cells in a UV-exposed region. Panel B shows the chlorophyll fluorescence (long pass of 650 nm) of these cells. In panel C is shown the accumulated fluorescein fluorescence (band-pass of 505−550 nm). The patterns of fluorescence in panels B and C are very consistent, showing that the vast majority of cells convert FDA and hence are viable. Bars are 50 μm long.

phosphatidic acid is not hydrolyzed *in vivo*. Probably, these cells are immobilized because they are stuck to the coverslip. On the other hand, in a region which is exposed to UV light for a short period of time (1 min), the phase contrast image (Figure 6B) shows that these cells do not carry their flagella anymore. Remarkably, some of the excised flagella can be observed in the phase contrast image.

Viability of Chlamydomonas Is Unaltered after UV Exposure. Experiments performed by UV exposure of nontreated cells or NPE-Ac-loaded cells indicate that the motility arrest of caged PtdOH-treated cells is not due to the phototoxicity or toxicity of the released cage. Still, to exclude the possibility that the arrest of swimming is due to processes other than the photorelease of PtdOH and subsequent deflagellation, we examined the cell viability of nonswimming cells. A useful marker for cell viability is fluorescein diacetate (FDA). FDA is a nonfluorescent esterified fluorescein which can be hydrolyzed by nonspecific esterase to brightly fluorescent fluorescein, indicating viable cells (*27*). To our knowledge, FDA has not been used as a viability marker for *Chlamydomonas*. To test whether FDA can be hydrolyzed in *Chlamydomonas* cells, 10 μM FDA was added to nontreated cells. This resulted in a fast (within 1 min) increase in intracellular green fluorescence, which is not observed in cells that are not incubated with FDA or in cells first fixed with 1.5% formaldehyde (data not shown). The green fluorescence can easily be separated from the chlorophyll fluorescence, by passing it through a band-pass filter at 505−550 nm. Chlorophyll is imaged with a LP650 nm long pass filter. By combining the results of the chlorophyll fluorescence with the FDA staining, we can estimate cell viability. These results show that hydrolysis of FDA can be used as a viability indicator for *Chlamydomonas* under standard conditions. This is in sharp contrast with the use of AM esters of calcium and pH probes which require special conditions (temperature of at least 30 °C and a medium pH lower than 5.5) to yield fluorescent algae (*28*).

Next, the viability after photorelease of PtdOH was examined. Cells incubated with caged PtdOH were exposed to UV light under a fluorescence microscope as performed previously. Directly after the UV exposure, an equal volume of a 20 μM FDA solution was added to the cells on the coverslip, and the fluorescein and chlorophyll fluorescence were imaged simultaneously (Figure 7). As can be inferred from Figure 7, the majority (>85%) of the cells that stopped swimming upon UV exposure exhibited green fluorescence, indicating that these cells are alive.

CONCLUSION

The structurally simple lipid phosphatidic acid is important in a great number of signaling cascades in both plant (*1*) and animal cells (*2*). To prove that PtdOH is sufficient for transducing a signal, we synthesized a photolabile precursor that can be incorporated into cells and subsequently release PtdOH by UV illumination. A fluorescently labeled derivative was prepared, allowing sensitive and convenient analysis of the uncaging process by TLC. The TLC analysis yielded a surprise as a stable intermediate is observed after incomplete photolysis. As it turns out, during synthesis the singly caged phosphodiester reacts another time, yielding a doubly caged PtdOH. It is known from the synthesis of DMNPE-caged cAMP and cGMP that the diazo compound can react with a phosphodiester (*14*). In a previous report of the synthesis of caged phosphatidic acid (*25*), the intermediate was not observed in the photolysis reaction. Possibly, the TLC solvent system that was used was not able to separate these compounds. We noted that the separation of the singly caged PtdOH from the doubly caged PtdOH was dependent on the solvent system (compare lanes C and F6 in Figure 2).

The novel assay for measuring the extent of uncaging of NPE_2-PtdOH in a fluorimeter greatly simplifies the determination of the uncaging quantum yield. We expect that this assay can be used for characterizing other (new) caged phospholipids, and for membrane-bound caged compounds in general. Moreover, this assay is not restricted to the classical nitrobenzyl based cages but can also be applied to other cages, such as the coumarin-based cages (*29*). These have relatively high extinction coefficients and therefore would be excellent quenchers of pyrene fluorescence.

It has been shown that adding phosphatidic acid at a millimolar concentration induces deflagellation of *Chlamydomonas* (*4*). This study shows that an at least 100-fold lower concentration of caged PtdOH can be effective, after loading and UV exposure, which could be explained by efficient loading of caged PtdOH into the cells. An advantage of using NPE_2-PtdOH with a fluorescent acyl chain is that loading into cells can be confirmed by fluorescence microscopy. However, at the low concentrations of fluorescently tagged

NPE_2-PtdOH that were used, we were not able to detect BODIPY fluorescence above the autofluorescence background in *Chlamydomonas* cells. Using similar concentrations of fluorescently tagged NPE_2-PtdOH in mammalian cells or in plant cells with less autofluorescence (e.g., root hairs lacking chlorophyll), it was possible to obtain images of fluorescent NPE_2-PtdOH in living cells (see the Supporting Information).

The low concentration of caged PtdOH that is able to elicit the deflagellation response provides evidence that PtdOH acts as a second messenger in its own right (*1*). Still, the downstream targets or effects of PtdOH leading to flagellar excision (e.g., calcium influxes) are unknown. We anticipate that photorelease of phosphatidic acid *in vivo* will be a valuable tool for studying the effect of PtdOH in a wide variety of signaling cascades.

APPENDIX

The reaction scheme of a doubly caged PtdOH undergoing photolysis to free PtdOH can be described with two consecutive uncaging reactions with rate constants k_1 and k_2:

$$c_2PA \xrightarrow[-NAP]{k_1} cPA \xrightarrow[-NAP]{k_2} PA \qquad (I)$$

In this reaction, c_2PA, cPA, PA, and NAP represent doubly caged PtdOH, singly caged PtdOH, free uncaged PtdOH, and the released side product nitrosoacetophenone, respectively. Differential equations describing the reaction kinetics of substrate decrease and product increase are

$$\frac{\partial[c_2PA]}{\partial t} = -k_1[c_2PA]$$

$$\frac{\partial[cPA]}{\partial t} = k_1[c_2PA] - k_2[cPA]$$

$$\frac{\partial[PA]}{\partial t} = k_2[cPA] \qquad (II)$$

$$\frac{\partial[NAP]}{\partial t} = k_1[c_2PA] + k_2[cPA]$$

The solutions describing the concentration of the substrate (which is initially c_0) and products at time t are

$$[c_2PA] = c_0 e^{-k_1 t}$$

$$[cPA] = c_0\left(\frac{k_1}{k_1 - k_2}\right)(e^{-k_2 t} - e^{-k_1 t})$$

$$[PA] = c_0\left[1 + \left(\frac{k_2}{k_1 - k_2}\right)e^{-k_1 t} - \left(\frac{k_1}{k_1 - k_2}\right)e^{-k_2 t}\right] \qquad (III)$$

$$[NAP] = \frac{c_0}{k_1 - k_2}[2 - k_1 e^{-k_2 t} - (k_1 - 2k_2)e^{-k_1 t}]$$

We assume that the uncaging rate will be proportional to the number of cages. Hence, it is assumed that $k_1 = 2k_2$. By substituting $k_2 \equiv k$ and $k_1 = 2k$, we reduce eq III to

$$[c_2PA] = c_0 e^{-2kt}$$

$$[cPA] = 2c_0(e^{-kt} - e^{-2kt})$$

$$[PA] = c_0(1 + e^{-2kt} - 2e^{-kt}) \qquad (IV)$$

$$[NAP] = 2c_0(1 - e^{-kt})$$

Our assay, described in Materials and Methods and schematically depicted in Figure 3A, measures quenching of a pyrene lipid by the NPE cage, and therefore, c_2PA and cPA both quench pyrene. Furthermore, we assume a residual quenching by the nitrosoacetophenone side product that is released upon uncaging.

Quenching of a fluorophore according to Stern−Volmer quenching by multiple compounds can be described as

$$F_0/F = 1 + \sum_i K_{Q_i}[Q_i] \qquad (V)$$

in which F_0 is the fluorescence in the absence of a quencher and F the fluorescence in the presence of a quencher with a concentration [Q] and a quenching constant K_Q.

$$F_0/F = 1 + K_{Q_1}[c_2PA] + K_{Q_2}[cPA] + K_{Q_3}[NAP] = 1 + 2K_{Q_3}c_0 + (K_{Q_2} - 2K_{Q_3})c_0 e^{-kt} \qquad (VI)$$

In eq VI, K_{Q_1}, K_{Q_2}, and K_{Q_3} are the quench constants of c_2PA, cPA, and NAP, respectively. It is assumed that due to the presence of two NPE cages c_2PA quenches the pyrene twice as efficiently as the singly caged cPA (i.e., $K_{Q_1} = 2K_{Q_2}$). Inverting eq VI yields eq 1 in Materials and Methods.

ACKNOWLEDGMENT

We thank Martine den Hartog and John van Himbergen (Plant Physiology, University of Amsterdam) for the continuous supply of fresh and happily swimming *C. moewusii* cells.

SUPPORTING INFORMATION AVAILABLE

Fluorescence images of mammalian and plant cells loaded with caged fluorescent PtdOH. This material is available free of charge via the Internet at http://pubs.acs.org.

REFERENCES

1. Munnik, T. (2001) Phosphatidic acid: an emerging plant lipid second messenger, *Trends Plant Sci. 6*, 227−233.
2. English, D. (1996) Phosphatidic acid: a lipid messenger involved in intracellular and extracellular signalling, *Cell Signalling 8*, 341−347.
3. Divecha, N., and Irvine, R. F. (1995) Phospholipid signaling, *Cell 80*, 269−278.
4. Munnik, T., Arisz, S. A., de Vrije, T., and Musgrave, A. (1995) G protein activation stimulates phospholipase D signaling in plants, *Plant Cell 7*, 2197−2210.
5. Jacob, T., Ritchie, S., Assmann, S. M., and Gilroy, S. (1999) Abscisic acid signal transduction in guard cells is mediated by phospholipase D activity, *Proc. Natl. Acad. Sci. U.S.A. 96*, 12192−12197.
6. Ritchie, S., and Gilroy, S. (1998) Abscisic acid signal transduction in the barley aleurone is mediated by phospholipase D activity, *Proc. Natl. Acad. Sci. U.S.A. 95*, 2697−2702.

7. Pagano, R. E., and Longmuir, K. J. (1985) Phosphorylation, transbilayer movement, and facilitated intracellular transport of diacylglycerol are involved in the uptake of a fluorescent analog of phosphatidic acid by cultured fibroblasts, *J. Biol. Chem. 260*, 1909−1916.
8. Alderton, F., Sambi, B., Tate, R., Pyne, N. J., and Pyne, S. (2001) Assessment of agonism at G-protein coupled receptors by phosphatidic acid and lysophosphatidic acid in human embryonic kidney 293 cells, *Br. J. Pharmacol. 134*, 6−9.
9. Jiang, T., Sweeney, G., Rudolf, M. T., Klip, A., Traynor-Kaplan, A., and Tsien, R. Y. (1998) Membrane-permeant esters of phosphatidylinositol 3,4,5-trisphosphate, *J. Biol. Chem. 273*, 11017−11024.
10. McCray, J. A., and Trentham, D. R. (1989) Properties and uses of photoreactive caged compounds, *Annu. Rev. Biophys. Biophys. Chem. 18*, 239−270.
11. Walker, J. W., Somlyo, A. V., Goldman, Y. E., Somlyo, A. P., and Trentham, D. R. (1987) Kinetics of smooth and skeletal muscle activation by laser pulse photolysis of caged inositol 1,4,5-trisphosphate, *Nature 327*, 249−252.
12. Gilroy, S., Read, N. D., and Trewavas, A. J. (1990) Elevation of cytoplasmic calcium by caged calcium or caged inositol triphosphate initiates stomatal closure, *Nature 346*, 769−771.
13. Kaplan, J. H. (1990) Photochemical manipulation of divalent cation levels, *Annu. Rev. Physiol. 52*, 897−914.
14. Nerbonne, J. M., Richard, S., Nargeot, J., and Lester, H. A. (1984) New photoactivatable cyclic nucleotides produce intracellular jumps in cyclic AMP and cyclic GMP concentrations, *Nature 310*, 74−76.
15. Adams, S. R., and Tsien, R. Y. (1993) Controlling cell chemistry with caged compounds, *Annu. Rev. Physiol. 55*, 755−784.
16. Munnik, T., de Vrije, T., Irvine, R. F., and Musgrave, A. (1996) Identification of diacylglycerol pyrophosphate as a novel metabolic product of phosphatidic acid during G-protein activation in plants, *J. Biol. Chem. 271*, 15708−15715.
17. Kuhn, H. J., Braslavski, S. E., and Schmidt, R. (1989) Chemical actinometry, *Pure Appl. Chem. 61*, 187−210.
18. Gupta, C. M., Radhakrishnan, R., and Khorana, H. G. (1977) Glycerophospholipid synthesis: improved general method and new analogs containing photoactivable groups, *Proc. Natl. Acad. Sci. U.S.A. 74*, 4315−4319.
19. Selinger, Z., and Lapidot, Y. (1966) Synthesis of fatty acid anhydrides by reaction with dicyclohexylcarbodiimide, *J. Lipid Res. 7*, 174−175.
20. Comfurius, P., and Zwaal, R. F. (1977) The enzymatic synthesis of phosphatidylserine and purification by CM-cellulose column chromatography, *Biochim. Biophys. Acta 488*, 36−42.
21. Walker, J. W., Reid, G. P., McCray, J. A., and Trentham, D. R. (1988) Photolabile 1-(2-nitrophenyl)ethyl phosphate esters of adenine nucleotide analogues. Synthesis and mechanism of photolysis, *J. Am. Chem. Soc. 110*, 7170−7177.
22. Walker, J. W., Reid, G. P., and Trentham, D. R. (1989) Synthesis and properties of caged nucleotides, *Methods Enzymol. 172*, 288−301.
23. Goedhart, J., Hink, M. A., Visser, A. J., Bisseling, T., and Gadella, T. W., Jr. (2000) In vivo fluorescence correlation microscopy (FCM) reveals accumulation and immobilization of Nod factors in root hair cell walls, *Plant J. 21*, 109−119.
24. Somerharju, P. J., Virtanen, J. A., Eklund, K. K., Vainio, P., and Kinnunen, P. K. (1985) 1-Palmitoyl-2-pyrenedecanoyl glycerophospholipids as membrane probes: evidence for regular distribution in liquid-crystalline phosphatidylcholine bilayers, *Biochemistry 24*, 2773−2781.
25. Williger, B. T., Reich, R., Neeman, M., Bercovici, T., and Liscovitch, M. (1995) Release of gelatinase A (matrix metalloproteinase 2) induced by photolysis of caged phosphatidic acid in HT 1080 metastatic fibrosarcoma cells, *J. Biol. Chem. 270*, 29656−29659.
26. Thuren, T., Virtanen, J. A., Somerharju, P. J., and Kinnunen, P. K. (1988) Phospholipase A2 assay using an intramolecularly quenched pyrene-labeled phospholipid analog as a substrate, *Anal. Biochem. 170*, 248−255.
27. Haugland, R. P. (1996) Handbook of fluorescent probes and research products. pp 679, Molecular Probes, Eugene, OR.
28. Braun, F. J., and Hegemann, P. (1999) Direct measurement of cytosolic calcium and pH in living *Chlamydomonas reinhardtii* cells, *Eur. J. Cell Biol. 78*, 199−208.
29. Furuta, T., and Iwamura, M. (1998) New caged groups: 7-substituted coumarinylmethyl phosphate esters, *Methods Enzymol. 291*, 50−63.

BI0351460